from where cancer cells had disappeared [1]. The application of this classification was extended to evaluation of chemotherapeutic effects in 1985 and adopted in the 11th edition of the General Rules for the Gastric Cancer Study [2]. However, it was very difficult to determine correctly whether the altered cancer cells were viable.

In the NSABP-B-18 trial of neoadjuvant chemotherapy for patients with breast cancer, a histopathological evaluation system for chemotherapeutic effects was adopted solely on the basis of the presence or absence of invasive cancer cells, regardless of the degree of cellular degeneration or viability [3]. Thereafter, in different histopathological criteria used for evaluating therapeutic effects in breast cancers by using neoadjuvant chemotherapy, the evaluation was done usually on the basis of the presence of residual tumor cells, regardless of the extent of alteration of residual cancer cells [4, 5]. Because the sensitivity of cancer cells against chemo- or radiotherapy differs among cases, and the extent of therapeutic effects was shown to be correlated with patients' prognosis, accurate histopathological assessment of therapeutic effects has come to be required by clinical oncologists to pathologists as a routine activity. Because sometimes the pathological complete response (pCR) is set as the primary end point of clinical studies of neoadjuvant therapies to breast cancers [6–8], evaluation is frequently conducted in the form of a central pathological review [7, 8].

Recently, radiofrequency ablation (RFA) has been introduced in the field of breast cancer therapy [9, 10]. Because the effect of RFA is evaluated by cautery effect, which is almost common among tumors if the conditions of operation were uniform, establishment of common criteria for assessing therapeutic effects would be very useful to pathologists. In general, evaluation is performed by a combination of hematoxylin and eosin (HE) staining and nicotinamide adenine dinucleotide (NADH)-diaphorase

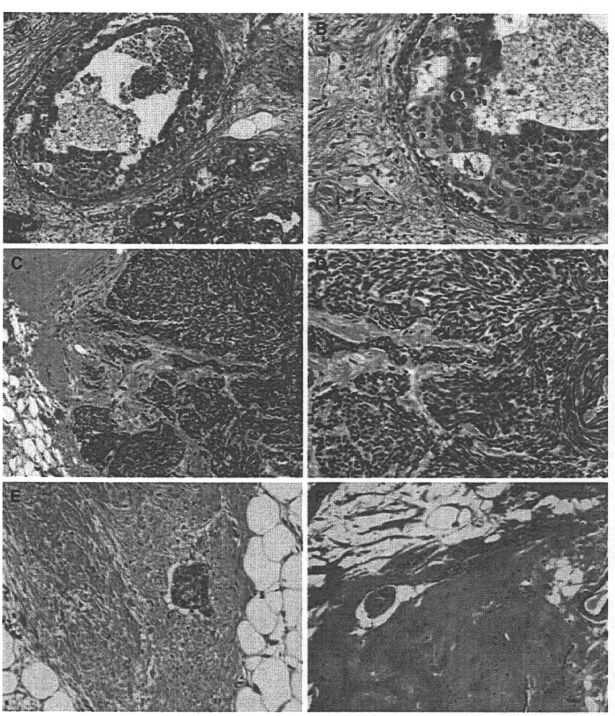


**Fig. 1** Alterations in breast cancer and noncancerous tissues by radiofrequency ablation (RFA). **a**, **b** In situ component of a ductal carcinoma without RFA effect. Cancer cells and stromal lymphocytes are viable without degenerative changes, and the morphology of stromal collagen fiber is well preserved. **c**, **d** Invasive carcinoma component with RFA effect. Cancer cells and stromal cells show pyknotic "streaming" nuclei, unclear intercellular boundaries, and unclear nuclear and cytoplasmic morphological details. In stroma, collagen fibers show degenerative changes. **e** Breast stromal tissue without RFA effect. The morphology of stromal collagen fibers is well preserved. A cancer cell nest is also seen. **f** Noncancerous stromal tissue with RFA effect. In stroma, collagen fibers show degenerative changes resulting in dense homogeneous and highly eosinophilic features. ×100 in **a**, **c**, **e**, and **f**, and ×200 in **b** and **d**. ×100 in **a** and **c**, and ×200 in **b** and **d**

staining (reviewed in ref. [11]). Although several studies have shown that evaluation of the therapeutic effects by using NADH-diaphorase staining is useful, evaluation of therapeutic effects by RFA would become more reproducible and accurate if evaluations are effectively done using HE-stained sections of formalin-fixed, paraffin-embedded tissues. Seki et al. [11] have described criteria for histopathological evaluation of RFA effects in breast cancers.

In the present study, RFA effects assessed by HE staining were compared with those assessed by NADH-diaphorase staining of surgically resected breast-cancer tissues, which were obtained immediately after RFA application in a pilot study to examine the safety and efficacy of RFA [9, 11]. In addition, we examined the parameters that caused suboptimal histopathological therapeutic effects in the tumor treated by RFA.

## Patients and methods

### RFA study protocol

This study was approved by the Institutional Review Board for ethical issues in the National Cancer Center, Japan. All the patients provided written informed consent. The criteria for patient selection and the RFA protocol have been previously described [9]. Under ultrasound guidance, RFA was performed using the 17-gauge Valleylab RF Ablation System with Cool-tip Technology (Covidien, Energy-Based Devices, Interventional Oncology, Boulder, CO) [9]. Histochemical and histopathological examinations of specimens from 28 patients who underwent RFA for primary breast cancer and subsequent partial breast resection or mastectomy between June 2008 and May 2009 were performed. For RFA, radiofrequency energy was sufficient in 19, but the increase of the energy during the procedure was suboptimal in 2 cases (cases 23 and 27 in Table 1).

After ablation, the surgically resected specimens were subjected to sampling of tumor and control tissues for NADH-diaphorase staining. From the representative cut surface of the ablated tumor, at least two thinly sliced sections 2–3 cm in size were removed and prepared as frozen sections: one section contained an apparently ablated area and a representative cut surface of the main tumor, and the other contained non-tumor areas without RFA effect. These tissues were mounted in Cryo Mount I (Muto Pure Chemicals, Tokyo, Japan), immediately frozen on dry ice, and cut into 8- to 10-μm-thick sections. One of these sections was stained with HE, and the others were stored at −80°C until NADH-diaphorase staining.

Enzyme histopathological analysis of the ablated breast tumors was performed according to a method described by Seki et al. [11] and Imoto et al. [12]. The ablated areas were confirmed to contain dead cells, which were negative for the oxidation-reduction reaction mediated by NADH-diaphorase, whereas residual live cells stained blue. We compared the histopathological features of the stained with the unstained adjacent areas by using serial sections stained with both the NADH-diaphorase reaction and HE. The histopathological features attributable to the thermal effects of RFA were investigated by two pathologists.

The remaining surgically resected specimens were fixed in 10% formalin and processed for routine histopathological examination. For partially resected breast specimens, a total of ~20–30 tissue blocks were all sectioned. For total mastectomy specimens, more than 15 tissue blocks were made, all including entire tumor areas. If necessary, additional cutting was performed after initial histological examinations. The ablated areas and ablated tumorous areas were mapped on cut sections, and on the basis of this map, the percentage areas containing tumorous tissue was estimated by at least 2 pathologists.

For both frozen sections and formalin-fixed, paraffin-embedded sections stained with HE, RFA damage to the epithelial cells and fibrous stroma was histologically evaluated according to the criteria described by Seki et al. [11]. In brief, the area with RFA effect in HE-stained sections was histologically visualized as follows (Fig. 1).

**Table 2** Summary of the profiles of 28 primary breast carcinomas subjected to radiofrequency ablation (RFA) and subsequent partial resection of the breast or mastectomy

| | |
|---|---|
| Mean tumor size (total) | 2.21 cm (0.6–5.0) (1.31 SD) |
| Mean tumor size (invasion) | 1.44 cm (0–5.0) (1.00 SD) |
| Mean size of degenerated area by RFA | 3.71 cm (1.7–6.0) (1.33 SD) |
| Incidence of 100% RFA effect by HE staining in primary tumor | 16/28 (57%) |
| Incidence of 100% RFA effect by NADH-diaphorase staining in primary tumors | 22/28 (79%) |
| Concordance between RFA effect by HE and RFA effect NADH-diaphorase staining | 22/28 (79%) |

Tumor size (total) includes both invasive and intraductal components

*HE* hematoxylin and eosin, *NADH* nicotinamide adenine dinucleotide, *SD* standard deviation

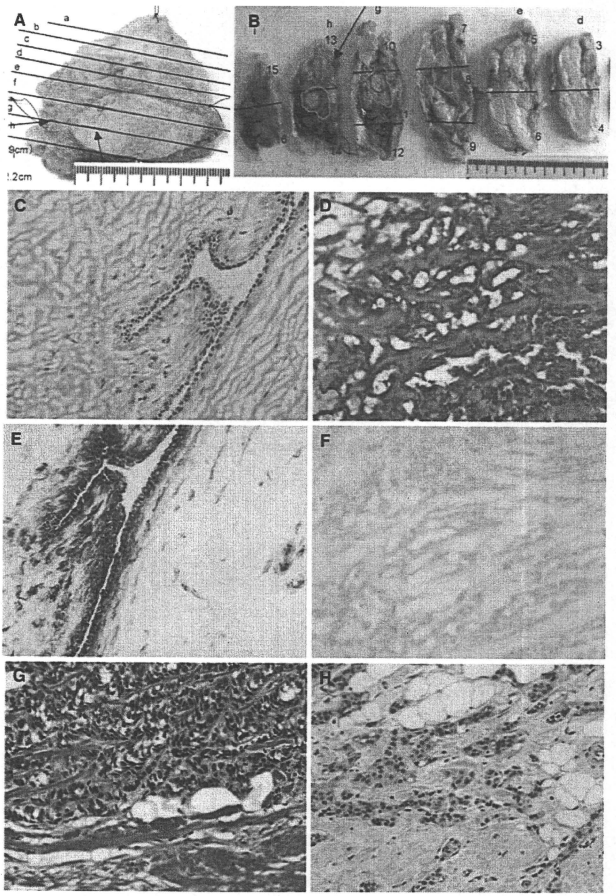


**Fig. 2** A case with 100% effective RFA in the main tumor but no effect in the daughter lesion assessed by hematoxylin and eosin (HE) staining. **a**, **b** Surgically resected specimens. *Areas* in *red* represent invasive carcinoma components. Ablated areas are circumscribed in *green*. An *arrow* indicates the daughter lesion. **c**, **d** Frozen sections of the resected tissue specimens stained with HE. **c** Viable non-tumor area with no histopathological RFA effect. No degradation changes are seen in epithelial cells and stromal structures. **d** Tumor area with a strong histopathological RFA effect. Tumor tissues had lost intercellular boundaries and nuclear or cytoplasmic morphological details. Fibrous connective tissue is also highly degenerated into a densely homogeneous and highly eosinophilic structure. **e**, **f** Nicotinamide adenine dinucleotide (NADH)-diaphorase reaction of serial sections of **c** and **d**. **e** NADH diaphorase in a histopathologically viable area. **f** NADH diaphorase in an area with highly degenerated histopathological features. **g**, **h** Permanent sections stained with HE. **g** Histopathologically highly degenerated tumor area (*upper*) and stromal area (*lower*). **h** Histopathological features of the daughter lesions in which no RFA effect is seen. ×100

Epithelial cells, both cancerous and noncancerous, were characterized by elongated eosinophilic cytoplasm with pyknotic "streaming" nuclei. The intercellular boundaries and details of the nuclear and cytoplasmic morphology were unclear (Fig. 1a–d). Fibrous connective tissue also showed degenerative changes with dense homogeneous and highly eosinophilic features. The original delicate, wavy appearance entirely disappeared. Fibroblasts in the area also showed thermal degenerative changes identical to those seen in epithelial cells (Fig. 1e, f).

### Statistical analysis

Statistical difference was analyzed by Fisher's exact test.

## Results

The findings of pathological examination of the 28 tumors subjected to RFA are presented in Tables 1 and 2. In the Tables, tumor size or tumor size (total) means to the largest

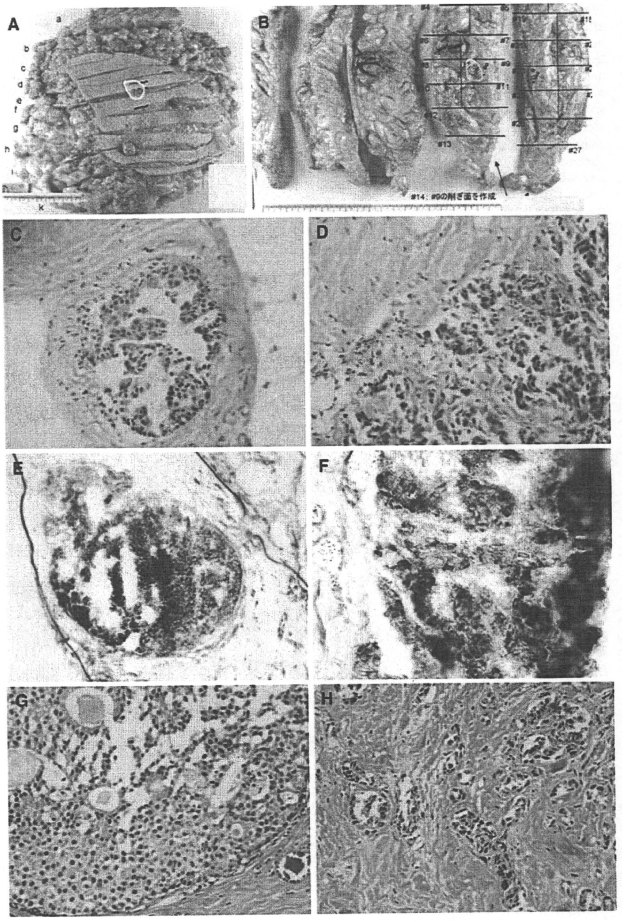


**Fig. 3** A case in which histological evaluation of RFA effect was 80% by HE, but the effect was absent by NADH-diaphorase staining. **a**, **b** Surgically resected specimens. *Areas* in *red* and *blue* represent invasive carcinoma and ductal carcinoma in situ (DCIS), respectively. Ablated areas are represented in *yellow*. **c**, **d** Frozen sections of the tumor tissue stained with HE. **c** A viable area without histopathological RFA effect. No degradation changes are seen in either tumor or stromal tissues. **d** An area with histopathological RFA effect. The cells of the tumor tissue show elongated eosinophilic cytoplasm with pyknotic nuclei. **e**, **f** NADH-diaphorase reaction. The results of NADH-diaphorase staining were positive in both histologically viable and nonviable tissue areas in series with **c** and **d**. **g**, **h** Formalin-fixed, paraffin-embedded sections stained with HE. **g** Histopathologically viable DCIS area. **h** Histopathologically highly degenerated invasive carcinoma area. Findings are the same as those in **d**; ×100 in **c** and **e**; ×200 in **d**, **f**, **g** and **h**

diameter of the tumor, including invasive carcinoma and intraductal carcinoma components and including both ablated and non-ablated tumor area. Histological grades of the tumors were 1, 2, and 3 in 18, 5, and 4, respectively. Grading of one tumor could not be determined because of marked degenerative changes. The mean tumor size, including both invasive and noninvasive components, was 2.21 cm, ranging from 0.6 to 5.0 cm. The mean size of invasive components was 1.44 cm, ranging from 0 [ductal carcinoma in situ (DCIS)] to 5.0 cm. An extensive intraductal component (EIC) was positive in 9 tumors, but negative in 17 tumors. One case of DCIS and one case of invasive ductal carcinoma with a predominantly DCIS component were included in the study.

The mean size of the degenerated areas by RFA, including both tumorous and the surrounding nontumorous

**Table 3** Factors correlated with 100% radiofrequency ablation (RFA) effect by hematoxylin eosin (HE) findings

| Factor | Number of tumors (%) RFA effect by HE | | | P |
|---|---|---|---|---|
| | Total | 100% Effect | <100% Effect | |
| Extensive intraductal component (EIC) | | | | |
| EIC(+) | 9 | 1 (11) | 8 (89) | 0.0022 |
| EIC(−) | 17 | 13 (76) | 4 (24) | |
| DCIS | 2 | 2 (100) | 0 (0) | |
| Tumor size (total, cutoff 1.5 cm)[a] | | | | |
| ≤1.5 cm | 11 | 10 (91) | 1 (9) | 0.0034 |
| >1.5 cm | 17 | 6 (35) | 11 (65) | |
| Tumor size (total, cutoff 1.0 cm and 2.0 cm) | | | | |
| ≤1.0 cm | 5 | 5 (100) | 0 (0) | 0.0037 |
| >1.0 cm, ≤2.0 cm | 11 | 8 (73) | 3 (27) | |
| >2.0 cm | 12 | 3 (25) | 9 (75) | |

Tumor size (total) includes both invasive and intraductal components

*DCIS* ductal carcinoma in situ, *EIC* extensive intraductal component

[a] One tumor of ≤1.5 cm but <100% RFA effect was 1.5 cm in diameter, and the effect was 95% by HE and 100% by NADH-diaphorase staining

tissues, was 3.71 cm, ranging from 1.7 to 6.0 cm. Incidence of a 100% effective RFA by HE was 57% (16 of 28) in primary tumors. Of these 16 cases, 1 had a daughter nodule, and because RFA was performed only for the main tumor, the therapeutic effect was 100% for the main tumor, but the effect was absent for the daughter nodule (Fig. 2). By HE, in tumors with incomplete RFA effect, the area of RFA effect was evaluated to be ≥90% in 6, whereas the area was evaluated to be <90% in 6, including 2 tumors (cases 23 and 27 in Table 1), which were potentially subjected to a suboptimal increase in energy during the RFA procedure.

Nicotinamide adenine dinucleotide-diaphorase staining was positive for all sections containing nonablated areas. In the ablated tissues, tumorous tissue, and surrounding non-tumorous tissue, the size of tumor detected by the NADH-diaphorase staining varied from 0.3 to 2.0 cm (mean 1.10 cm). The incidence of 100% effective RFA detected by NADH-diaphorase staining was 79% (22 of 28) in the primary tumors. The therapeutic effect evaluated by NADH-diaphorase staining was 100% in 22 tumors, <100% but ≥90% in 3 tumors. For the other 3 tumors, the RFA effect evaluated by NADH-diaphorase staining was ≤80%: 2 of these were patients 23 and 27, in whom the radiofrequency energy did not increase optimally. In case 27, histological evaluation of the RFA effect was 80% by HE, but the effect was absent by NADH-diaphorase staining because the results of the latter staining were positive in the entire specimen examined (Fig. 3). Concordance between HE findings and NADH findings of the RFA effect was 79% (22 of 28). The specificity and sensitivity of NADH-diaphorase results (complete or incomplete RFA effect) to HE results (complete or incomplete RFA effect) were 100% (16 of 16) and 50% (6 of 12), respectively.

A 100% effective RFA evaluated by HE staining was correlated with EIC(−) and tumor size (Table 3). A 100% effective RFA was observed in 13 (76%) of the 17 EIC(−) tumors, whereas a 100% effective RFA was observed in only 1 (11%) of the 9 EIC(+) tumors ($P = 0.0022$; Fig. 4). Two cases of DCIS showed 100% RFA effect.

Likewise, a 100% effective RFA evaluated by HE staining was correlated with tumor size, including intraductal component (Table 3): a 100% effective RFA was observed in 10 (91%) of 11 tumors of ≤1.5 cm in diameter, whereas a 100% effective RFA was observed in only 6 (35%) of 17 tumors of >1.5 cm in diameter ($P = 0.0034$). One case of ≤1.5 cm, but <100% effective RFA was 1.5 cm in diameter, and the effect was observed in 95% of the area by HE and 100% of the area by NADH-diaphorase staining.

When tumor size, including intraductal component, was stratified into three categories, 100% effects of RFA were detected in all 5 (100%), 3 (27%) of 11, and 9 (75%) of 12 in tumor groups of tumor size ≤1.0 cm, >1.0 cm but ≤2.0 cm, and >2.0 cm, respectively (Table 3). The rate of a 100% effect of RFA was significantly higher in the patients with a tumor of ≤1.0 cm in size than in those with a tumor of >1.0 cm ($P = 0.0037$).

## Discussion

In this study, we evaluated the RFA effect by both HE and NADH-diaphorase staining in 28 primary breast cancers resected from patients immediately after RFA procedures. As studied by Seki et al. [11], therapeutic effects of RFA evaluated by HE were mostly concordant with the loss of cellular viability evaluated by NADH-diaphorase staining. Because the area examined in HE-stained sections was wider (2.21 cm on an average) than the area examined in NADH-diaphorase-stained sections (1.10 cm on an average), the percentage of 100% effective RFA became lower in the former (57%) than in the latter (79%). In 1 case (case 27), there was a discrepancy in the RFA effect between the HE and NADH staining in frozen sections, but examinations of the tumor tissue in formalin-fixed sections stained with HE revealed that HE findings were concordant between frozen sections and the formalin-fixed ones. From these results, only frozen-sectioning examination did not completely and accurately clarify the status of the RFA effect in the entire tumor tissue.

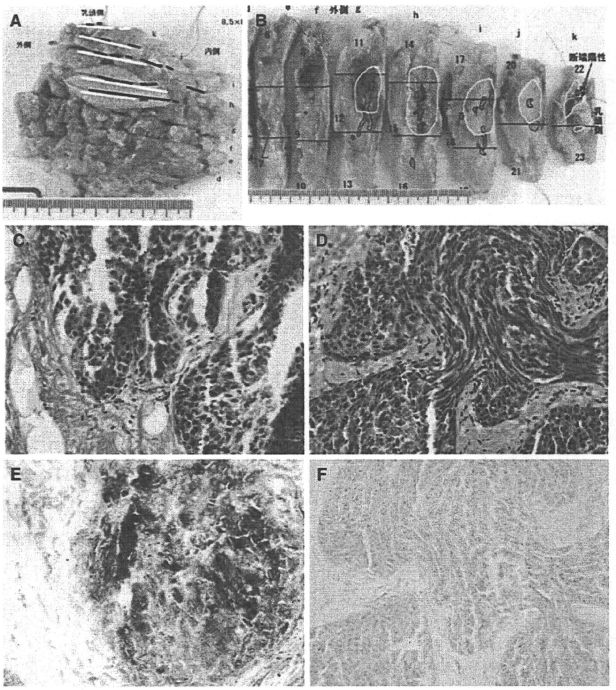


**Fig. 4** A case of breast carcinoma, extensive intraductal component (EIC)(+), with 60% effective RFA detected by HE staining of the sections. **a, b** Surgically resected specimens. *Areas* in *red* and *blue* represent invasive carcinoma and DCIS, respectively. Ablated areas are represented in *yellow*. **c, d** Frozen sections of the tumor tissue stained with HE. **c** Viable area without histopathological RFA effect. No degradative changes are seen in both tumor and stromal tissues. **d** An area with histopathological RFA effect. The cells of the tumor tissue show elongated eosinophilic cytoplasms with pyknotic "streaming" nuclei, unclear intercellular boundaries, and unclear morphological details in the nuclear or cytoplasmic features. Fibrous connective tissue also shows degenerative changes, resulting in dense homogeneous and highly eosinophilic features. **e, f** NADH-diaphorase reaction. **e** The results of NADH-diaphorase staining in histopathologically viable areas are positive. **f** NADH diaphorase in the area with histopathological RFA effect shows no reaction. ×200

Nonetheless, if the tumor size was small (≤1.5 cm) and the tumor lacked the EIC component, the proportion of cases with complete RFA effect became very high. In particular, complete RFA effects were observed in all tumors with a diameter of ≤1.0 cm. In these cases, if RFA therapy was conducted with subsequent follow-ups, examination of the therapeutic effect by means of core-needle/mammotome biopsy would be potentially sufficient. In contrast, the ratio of suboptimal RFA effect was high in the tumors sized 2.0 cm or larger. Even in the tumors of >1.0 cm but ≤2.0 cm in size microscopically, 27% of cases did not show a 100% of RFA effect. From the present data, tumor size of ≤1.5 cm, strictly ≤1.0 cm, could be an indication for RFA if a complete histological therapeutic effect is mandatory.

There are still challenges in determining the therapeutic effects of RFA. Judgments of the RFA therapeutic effects between HE and NADH-diaphorase staining, even by examining serial tissue sections, do not always agree. In the Chiba Cancer Center, RFA therapy and subsequent follow-up revealed cases in which HE findings showed effectiveness, but the results of NADH-diaphorase staining were positive, or cases in which HE showed no changes but the results of NADH-diaphorase staining were negative (Yamamoto N., personal communication). Data acquisition from a larger number of cases and establishment of uniform criteria for evaluation of histopathology determining therapeutic RFA effects, including researching on how the NADH-diaphorase findings should be incorporated into such criteria, are important next stages of research.

From Table 1, the diameter of the area with a RFA effect usually exceeds the tumor size by several times, including the intraductal component. The effect of RFA appeared to extend in a radial direction. We need to be concerned about the effects of this technique on the superficial and deep sides of the mammary gland. Histologically, 1 of 28 patients suffered ulceration by the heat injury on the overlying skin (no. 3 in Table 1). Pectoral

muscle was not resected in any of the patients, but in 11 of the 28 patients, the deepest area of the resected specimen widely showed a RFA effect (e.g., Fig. 4). In these patients, it is unclear if thr pectoral muscle suffered significant injury from RFA, and close follow-up is necessary.

**Acknowledgments** This work was supported in part by a grant-in-aid for scientific research from the Ministry of Health, Labor, and Welfare.

**Conflict of interest** The authors and their immediate family members have no conflicts of interest.

## References

1. Shimosato Y. Histopathological studies on irradiated lung tumors. Gann. 1964;55:521–35.
2. Japanese Research Society for Gastric Cancer. The general rules for the gastric cancer study. The 11th edition. Tokyo: Kanehara Shuppan; 1985. pp. 126–35.
3. Fisher B, Brown A, Mamounas E, Wieand S, Robidoux A, Margolese RG, et al. Effect of preoperative chemotherapy on local-regional disease in women with operable breast cancer: findings from National Surgical Adjuvant Breast and Bowel Project B-18. J Clin Oncol. 1997;15:2483–93.
4. Kuroi K, Toi M, Tsuda H, Kurosumi M, Akiyama F. Issues in the assessment of pathologic effect of primary systemic therapy for breast cancer. Breast Cancer. 2006;13:38–48.
5. Kuroi K, Toi M, Tsuda H, Kurosumi M, Akiyama F. Unargued issues on the pathological assessment of response in primary systemic therapy for breast cancer. Biomed Pharmacother. 2005; 59(Suppl 2):S387–92.
6. Buzdar AU, Ibrahim NK, Francis D, Booser DJ, Thomas ES, Theriault RL, et al. Significantly higher pathologic complete remission rate after neoadjuvant therapy with trastuzumab, paclitaxel, and epirubicin chemotherapy: results of a randomized trial in human epidermal growth factor receptor 2-positive operable breast cancer. J Clin Oncol. 2005;23:3676–85.
7. Mukai H, Watanabe T, Mitsumori M, Tsuda H, Nakamura S, Masuda N, et al. Final analysis of a safety and efficacy trial of preoperative sequential chemo-radiation therapy for the nonsurgical treatment (NST) in early breast cancer (EBC): Japan Clinical Oncology Group trial (JCOG0306). J Clin Oncol. 2010;28:7s (abstract).
8. Toi M, Nakamura S, Kuroi K, Iwata H, Ohno S, Masuda N, et al. Phase II study of preoperative sequential FEC and docetaxel predicts of pathological response and disease free survival. Breast Cancer Res Treat. 2008;110:531–9.
9. Kinoshita T, Iwamoto E, Tsuda H, Seki K. Radiofrequency ablation as local therapy for early breast carcinomas. Breast Cancer. 2010. doi:10.1007/s12282-009-0186-9.
10. Yamamoto N, Fujimoto H, Nakamura R, Arai M, Yoshii A, Kaji S, et al. Pilot study of radiofrequency ablation therapy without surgical excision for T1 breast cancer: evaluation with MRI and vacuum-assisted core needle biopsy and safety management. Breast Cancer. 2010. doi:10.1007/s12282-010-0197-6.
11. Seki K, Tsuda H, Iwamoto E, Kinoshita T. Histopathological effect of radiofrequency ablation therapy for primary breast cancer, with special reference to changes in cancer cells and stromal structure and a comparison with enzyme histochemistry. Breast Cancer. 2010. doi:10.1007/s12282-010-0215-8.
12. Imoto S, Wada N, Sakemura N, Hasebe T, Murata Y. Feasibility study on radiofrequency ablation followed by partial mastectomy for stage I breast cancer patients. Breast. 2009;18:130–4.

Breast Cancer (2011) 18:18–23
DOI 10.1007/s12282-010-0215-8



# Histopathological effect of radiofrequency ablation therapy for primary breast cancer, with special reference to changes in cancer cells and stromal structure and a comparison with enzyme histochemistry

**Kunihiko Seki · Hitoshi Tsuda · Eriko Iwamoto · Takayuki Kinoshita**

Received: 7 April 2010 / Accepted: 7 June 2010 / Published online: 4 August 2010


**Abstract** Radiofrequency ablation (RFA) therapy is expected to be applicable to small breast cancers, but no criteria for its histopathological effect have yet been established. Using samples obtained from 15 patients who had undergone RFA and subsequent mastectomy, we compared the histopathological changes in the ablated area with the results of histochemical staining based on the reduction of nitroblue tetrazolium chloride (NBT) by nicotinamide adenine dinucleotide (NADH) diaphorase in frozen tissue sections, and looked for histological changes indicative of the effect of RFA on breast cancer. Grossly, the ablated area in most of the tumors was rough, gritty, less moist, and surrounded by a red congestive limbic zone. The ablated area showed no staining by the NADH diaphorase reaction, and cancer cells in the area showed marked destruction characterized by an unclear intercellular boundary, elongated eosinophilic cytoplasm, pyknotic "streaming" nuclei, and a poorly defined nuclear and cytoplasmic texture. At the same time, fibrous connective tissue also showed degenerative changes, becoming densely homogeneous with loss of its delicate wavy structure. The area in which RFA appeared to have been histopathologically effective was mostly concordant with the area in which the NADH diaphorase reaction was negative. In the periphery of the ablated area, however, cellular changes caused by RFA were less marked, although the NADH diaphorase reaction was visualized with NBT. A larger number of cases should be examined in order to establish criteria for the histopathological effect of RFA on breast cancer.

**Keywords** Breast cancer · Radiofrequency ablation therapy · NADH diaphorase reaction · Histopathological criteria for therapeutic effect

K. Seki (✉)
Clinical Laboratory Division, JR Tokyo General Hospital, 2-1-3 Yoyogi, Shibuya-ku, Tokyo 151-8528, Japan
e-mail: kunihiko-seki@jreast.co.jp

K. Seki · H. Tsuda
Diagnostic Pathology Division, National Cancer Center Hospital, Tokyo, Japan

E. Iwamoto
Diagnostic Radiology Division, National Cancer Center Hospital, Tokyo, Japan

T. Kinoshita
Breast Surgery Division, National Cancer Center Hospital, Tokyo, Japan

## Introduction

Radiofrequency ablation (RFA) therapy is expected to be applicable to small breast cancers as an effective and safe curative treatment of choice. However, no criteria for defining its therapeutic effect have yet been established. The majority of previous studies have employed histopathological examination of hematoxylin–eosin (HE)-stained sections and the histochemical technique for visualizing the reduction of nitroblue tetrazolium chloride (NBT) by nicotinamide adenine dinucleotide (NADH) diaphorase in frozen sections.

The NAD+/NADH redox reaction is one of the most important in living biologic systems. NADH diaphorase activity judged from the reduction of NBT to formazan via oxidation of NADH is a reliable marker of cell viability. Assay of NADH diaphorase is performed histochemically using fresh frozen tissue sections. When reduced NADH is

oxidized by NADH diaphorase, free electrons are transferred to NBT, which becomes reduced and converted to the blue, water-insoluble dye formazan (Fig. 1). NADH diaphorase becomes bound to the structural components of the cell, thereby permitting histochemical visualization of its intracellular location by the use of NBT. Only viable cells have active diaphorase, whereas this activity seems to subside immediately after cell death.

On the other hand, several previous reports have described criteria for evaluation of the RFA effect. Jeffrey et al. [1] considered the presence of pyknotic nuclei and increased intensity of eosinophilic staining to be characteristics of tissue cautery due to heating. Earashi et al. [2] applied histopathological criteria for assessment of therapeutic response described in the "General Rules for Clinical and Pathological Recording of Breast Cancer". However, no histopathological criteria for the therapeutic effect of RFA have yet been established.

In the present study, on the basis of a comparison of histopathological changes in the ablated area with the results of histochemical assay with NADH diaphorase, we attempted to characterize the histological changes in breast cancer induced by RFA.

## Patients and methods

### RFA study protocol

Patient selection and the RFA protocol have been described previously [3]. Histochemical and histopathological examinations were performed on specimens from 15 patients who had undergone RFA for primary breast cancer and subsequent mastectomy between June 2006 and May 2007.

### Pathological analysis

After ablation, the surgically resected specimen was cut at the maximum diameter of the ablated breast tumor (Fig. 2). Both the ablated and non-ablated areas of each tumor and adjacent tissue were grossly evaluated, focusing particularly on the features of coagulation, congestion, and elasticity. Slices of tissue, each including apparently ablated and non-ablated areas, were obtained and mounted in optimal cutting temperature (OCT) compound. The tissue was then immediately frozen in liquid nitrogen, and cut into sections 8- to 10-μm thick. One of these sections was immediately stained with HE, and the others were stored at −80°C until NADH diaphorase-NBT studies. The remaining surgically resected specimens were fixed in 10% formalin and processed for routine histopathological examination.

### Enzyme histochemical analysis

For enzyme histopathological analysis of ablated breast tumors, frozen tissue sections were incubated for 1 h at 37°C in a solution consisting of 0.8 mg/mL reduced β-NADH (Sigma), 0.5 mg/mL nitroblue tetrazolium (Sigma), and 0.05 M Tris-buffered saline (pH 7.4) (Fig. 3). Each slide was fixed in 10% formalin for 30 min and washed in distilled water for 2 min, then glass coverslips were applied with an aqueous medium.

### Mapping and evaluation

Ablated cells were confirmed to be non-viable by their negativity for the oxidation–reduction reaction mediated by NADH diaphorase, whereas residual viable cells were stained blue. By referring to serial sections stained with

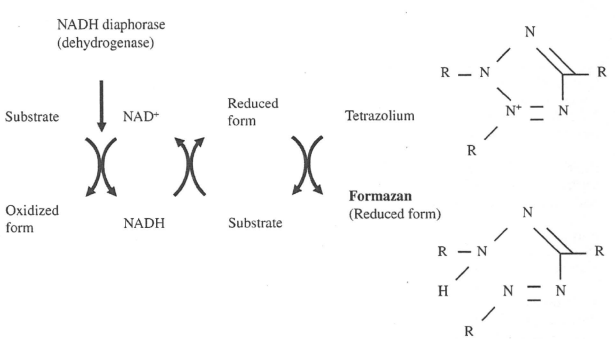


**Fig. 1** Nicotinamide adenine dinucleotide (NADH) redox circuit

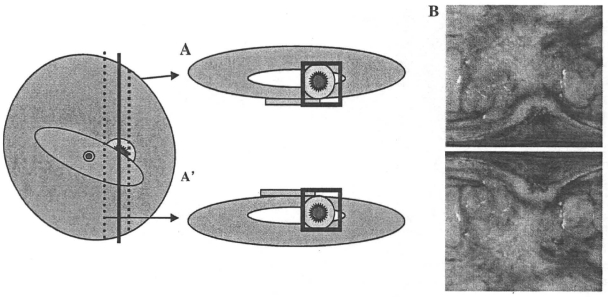


**Fig. 2** Schematic representation of tissue specimens used for evaluation of the histopathological effect of radiofrequency ablation (RFA) to primary breast cancer. **a** An ablated tumor cut at the maximum diameter. The tumor in cut section **a** is taken for NADH diaphorase staining. The tumor in cut section **a'**, the mirror image of section **a**, is taken for routine formalin-fixed and paraffin-embedded blocks. **b** Gross features of the ablated tumor. A congestive limbic zone encircles the ablated area containing the tumor

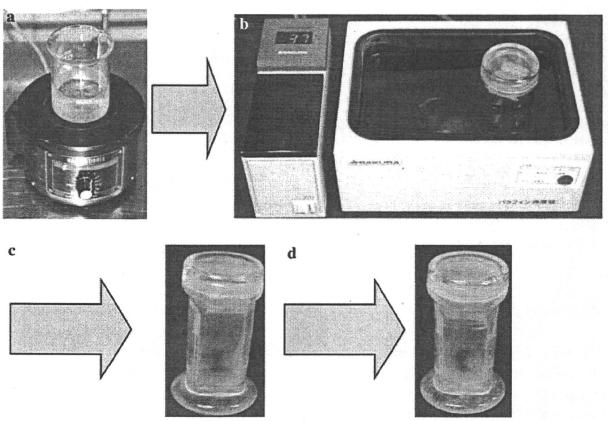


**Fig. 3** Preparation of reagents for histochemical assay of nicotinamide adenine dinucleotide (NADH) diaphorase activity. **a** Adjustment of NADH medium. The incubation medium consists of 0.8 mg/mL reduced $\beta$-NADH (Sigma), 0.5 mg/mL nitroblue tetrazolium, and 0.05 M Tris-buffered saline (pH 7.4), mixed at 37°C. **b** Fresh frozen tissue sections are incubated in the NADH medium in a water bath at 37°C for 1 h. **c** The tissue sections are washed in distilled water for 2 min. **d** These sections are subsequently fixed in 10% formalin for 30 min

both the NADH diaphorase reaction and HE, we compared the histopathological features of stained and adjacent non-stained areas. Gross and histological features attributable to the thermal effects of RFA were investigated by two pathologists (K.S. and H.T.).

## Results

### Gross examination

At the cut surface including the tumor, the ablated area felt firmer and more fragile than the surrounding non-ablated area. The cut surface of the ablated area composed of tumor and fibrous stroma was rough, gritty, and less moist, forming a round, flat surface surrounded by swollen fresh, unablated mammary, and fibroadipose tissue (Fig. 4a). In the central zone of the ablated area, the tumor and fibrous connective tissue were grayish-white to tan in color, forming a fissure or small cavity around the needle track (Fig. 4a). Coagulated non-tumor fibroadipose tissue was also firm and had changed to a tan-yellowish color. A red congestive limbic zone surrounded the ablated area (indicated with dots in Fig. 4a). These congestive rings were observed in 14 of 15 cases.

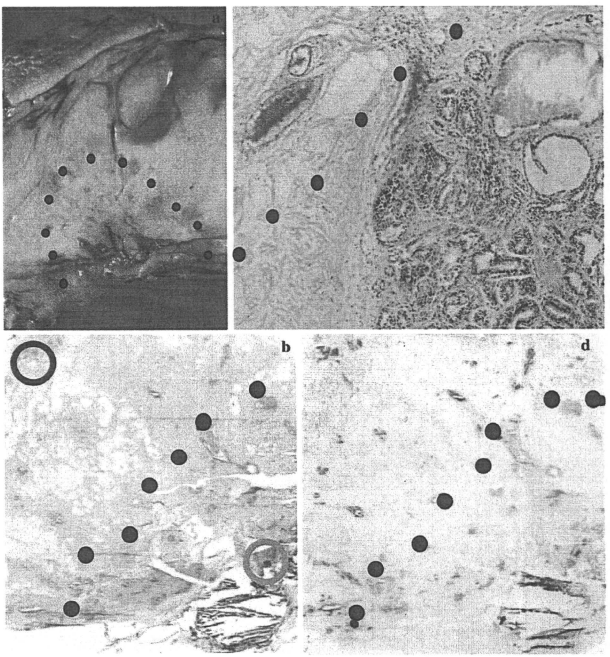


**Fig. 4** Macro- and microscopic features of RFA-treated breast cancer and non-cancerous tissue. **a** Gross features of a mastectomized specimen resected immediately after the RFA procedure. The border between the ablated and non-ablated areas is delineated by a congestive limbic zone (indicated by *dots*). **b** The boundary between the ablated area (*right lower* to *dots*) and non-ablated area (*left upper* to *dots*). A low-magnification view of an HE-stained section. The control part of the ablated area (*red circle*) shows highly degenerative changes. **c** A higher-magnification view of the boundary between the ablated (*right lower* to *dots*) and non-ablated (*left upper* to *dots*) areas. In the latter, congestive blood vessels are evident. In the former, mammary tissue and stroma with mild to moderate heating effects are observed (HE). **d** The boundary between the ablated and non-ablated areas in the serial section of image **b**. The section was subjected to the NADH diaphorase reaction to color viable cells blue due to the reduction of NBT. Only the non-ablated area (*left upper* to *dots*) is stained blue

## Microscopy examination

The boundary between the ablated and non-ablated area was identifiable histologically, although the effect of cautery showed a gradation from strong in the center to mild or moderate at the periphery (Fig. 4b, c). RFA damage to the epithelial cells and fibrous stroma in the ablated area was histologically visualized as follows in HE-stained sections. Epithelial cells, both cancerous and non-cancerous, were characterized by elongated eosinophilic cytoplasm with pyknotic "streaming" nuclei (Fig. 5b). The intercellular boundary and details of the nuclear and cytoplasmic texture were unclear. Fibrous connective tissue also showed degenerative changes resulting in dense homogeneous and highly eosinophilic features (Fig. 6). The original delicate, wavy structure had entirely disappeared. Fibroblasts in the area also showed thermal degenerative changes identical to those seen in epithelial cells.

At the periphery of the ablated area, epithelial cells showed coarse and plain nuclear chromatin due to the thermal effect (Fig. 5c). The boundary between ablated and non-ablated areas was usually characterized by congestive blood vessels, which were grossly evident as a red limbic zone (Fig. 4a). The effects of heating were sometimes relatively mild to moderate near the limbic zone, because the nuclear and cytoplasmic features characteristic of cell death at the periphery of the ablated area adjacent to the red zone were less marked (Fig. 5c) than those in the central ablated area.

## Comparison between NADH diaphorase reaction and histopathological findings

Nicotinamide adenine dinucleotide diaphorase-stained sections showed no reaction in tumor cells at the center of the ablated area, where tumor cells and stroma showed marked heat degeneration. The border between the NADH diaphorase-positive and -negative areas was relatively clear and sharp (Fig. 4d). NADH-positive cells showed the fine structures of intact nuclear chromatin and cytoplasm

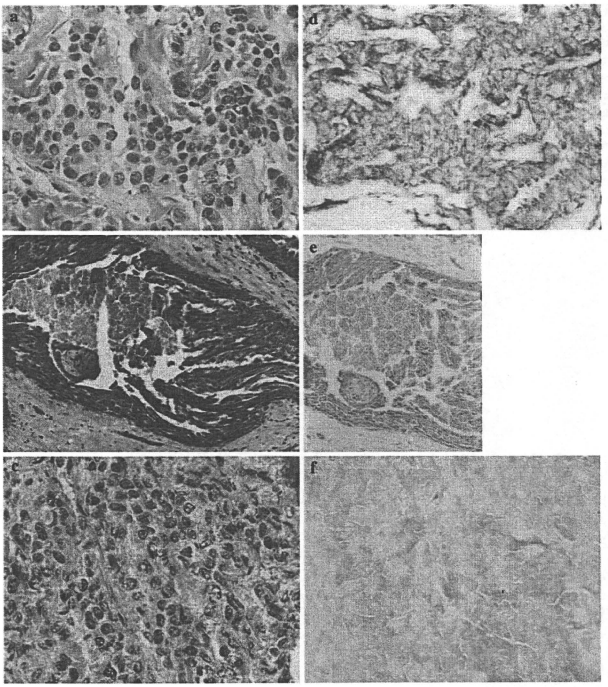


**Fig. 5** Comparison of histopathological features of RFA-treated breast cancer tissue with histochemical results of NADH diaphorase staining. **a, d** A non-ablated invasive ductal carcinoma (control specimen). **b, e** An invasive ductal carcinoma showing a strong effect of RFA cautery. **c, f** An invasive ductal carcinoma showing a moderate heating effect of RFA. **a** Fine structure of the nuclei and cytoplasm of tumor cells, and the collagen fibers of the stoma, are preserved. **b** Ablated tumor cells show an elongated cytoplasm with "streaming-like" nuclei. **c** Ablated tumor cells are characterized by pale cytoplasm and rough chromatin in the nuclei with an unclear cellular border. **d** This carcinoma shows a positive NBT reduction reaction, staining the cells blue, indicating histochemical positivity for NADH diaphorase activity. **e** This carcinoma shows a negative reaction for NADH diaphorase, indicating an absence of viable tumor cells. An invasive ductal carcinoma showing a strong cautery effect of RFA. **f** This carcinoma shows a negative reaction for NADH diaphorase, indicating an absence of viable tumor cells

(Fig. 5a, b), surrounded by a fine, delicate fibrous stroma. In each tumor, the NADH-negative area was approximately equivalent to the area circumscribed by the congestive limbic zone. Neither the central area showing strong effects of cautery, nor the peripheral part of the ablated area showing less marked effects showed the NADH diaphorase reaction (Fig. 5d, f).

## Discussion

We have described the macro- and microscopic findings characteristic of the cautery or heating effect of RFA, based on examination of specimens resected immediately after the procedure. The histopathological features of cellular damage described by some authors have included an unclear intercellular boundary, elongated eosinophilic cytoplasm, pyknotic "streaming" nuclei, and poorly defined nuclear and cytoplasmic texture [1, 4]. In addition, we found that the RFA procedure caused fibrous connective tissue to lose its delicate wavy structure and to degenerate to dense eosinophilic tissue with a loss of fine structure.

The area in which RFA was histologically effective was mostly concordant with the area of NADH diaphorase negativity, especially in the central part of the ablated area. At the periphery, however, cellular change caused by RFA was less marked, and the NADH diaphorase reaction visualized by NBT was usually negative. Fornage et al. described the histopathological changes observed in RFA-treated breast tissues in a study of 21 patients. The changes were similar to those observed in the present study, and were concordant with the results of NADH diaphorase staining [4]. However, a large number of cases should be studied in order to establish criteria for the histopathological effect of RFA. Although the histochemical assay for NADH diaphorase activity is reliable, it cannot always be performed in routine practice. It will therefore be necessary

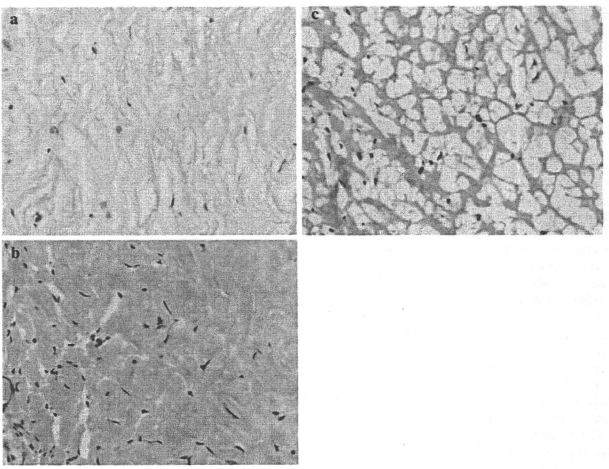


**Fig. 6** **a** Non-ablated stromal tissue in the breast demonstrates the fine wavy structure of collagen fibers (control specimen). **b, c** A highly ablated stroma showing eosinophilic and amorphous features without a fine wavy texture. Nuclei of fibroblasts are also pyknotic

to standardize criteria for the effects of RFA that are applicable to formalin-fixed and paraffin-embedded tissue sections.

**Acknowledgments** This work was supported in part by a grant-in-aid for scientific research from the Ministry of Heath, Labor and Welfare, Japan.

## References

1. Jeffrey SS, Birdwell RL, Ikeda DM. Radiofrequency ablation of breast cancer: first report of an emerging technology. Arch Surg. 1999;134:1064–8.
2. Earashi M, Noguchi M, Motoyoshi A, Fujii H. Radiofrequency ablation therapy for small breast cancer followed by immediate surgical resection or delayed mammotome excision. Breast Cancer. 2007;14:39–47.
3. Kinoshita T, Iwamoto E, Tsuda H, Seki K (2010) Radiofrequency ablation as local therapy for early breast carcinomas. Breast Cancer. doi:10.1007/s12282-009-0186-9
4. Fornage BD, Sneige N, Ross MI, Mirza AN, Kuere HM, Edeiken BS, et al. Small (≤2-cm) breast cancer treated with US-guided radiofrequency ablation: feasibility study. Radiology. 2004; 231:215–24.

Breast Cancer (2011) 18:10–17
DOI 10.1007/s12282-009-0186-9



# Radiofrequency ablation as local therapy for early breast carcinomas

**Takayuki Kinoshita · Eriko Iwamoto · Hitoshi Tsuda · Kunihiko Seki**

Received: 21 July 2009 / Accepted: 26 October 2009 / Published online: 14 January 2010


**Abstract**
*Purpose* To evaluate the safety and efficacy of radiofrequency ablation (RFA) as a local therapy for early breast carcinomas, we performed a phase I/II study at our institution.
*Patients and methods* Fifty patients with core-needle biopsy-proven breast carcinoma that was ≤3 cm in diameter on ultrasonography were enrolled in this study. Under ultrasound (US) guidance, the tumor and surrounding breast tissue were ablated with a saline-cooled RF electrode followed by immediate surgical resection. Resected specimens were examined by hematoxylin and eosin (H&E) staining and nicotinamide adenine dinucleotide (NADH) diaphorase staining to assess tumor viability.
*Results* Forty-nine patients completed the treatment. The mean tumor size was 1.70 cm. The mean ablation time was 8.7 min using a mean power of 48.5 W. Of the 49 treated patients, complete ablation was recognized in 30 patients (61%) by H&E staining and/or NADH diaphorase staining. The NADH viability staining was available for 38 patients, and in 29 (76.3%), there was no evidence of viable malignant cells. Of the 29 treated patients with breast carcinomas ≤2 cm in diameter examined by pathological examination, complete ablation was achieved in 24 patients (83%). Of the 26 treated patients with breast carcinomas without an extended intraductal component (EIC) according to pathological examination, complete ablation was determined in 22 patients (85%). RFA-related adverse events were observed in five cases: two with skin burn and three with muscle burns.
*Conclusion* RF ablation is a safe and promising minimally invasive treatment for small breast carcinomas with pathological tumor size ≤2 cm in diameter and without EIC.

**Keywords** Radiofrequency ablation · Local therapy · Early breast carcinomas · Phase I/II study

## Introduction

There has been a change in the management of cancer patients with localized disease from total mastectomy to lumpectomy complemented by adjuvant radiotherapy and chemo-endocrine therapy, without significant outcome [1, 2]. Early detection of small breast lesions may further change the attitude toward less invasive and even non-invasive management [3].

A major goal of breast-conserving treatment is the preservation of a cosmetically acceptable breast. Although a variety of patient and treatment factors have been reported to influence the cosmetic results, the amount of breast tissue resected appears to be a major factor [4]. Several investigators are studying the feasibility of percutaneous minimally invasive techniques to ablate breast tumors. Several modalities, such as cryosurgery, laser ablation, thermoablation, and high-intensity focused US, have been investigated [5]. By minimizing damage and

T. Kinoshita (✉) · E. Iwamoto
Surgical Oncology Division, National Cancer Center Hospital, 5-1-1 Tsukiji, Chuo-ku, Tokyo 104-0045, Japan
e-mail: takinosh@ncc.go.jp

H. Tsuda
Diagnostic Pathology Division, National Cancer Center Hospital, 5-1-1 Tsukiji, Chuo-ku, Tokyo 104-0045, Japan

K. Seki
Department of Pathology, JR Tokyo General Hospital, Tokyo, Japan

disruption to normal surrounding tissue, the morbidity of local treatment, such as scarring and deformity, can be reduced, and the cosmetic results can potentially be improved. With the widespread application of screening mammography, the mean size of the breast tumors detected has continued to decrease, which further emphasizes the need for less invasive means for achieving local tumor destruction, such as RF ablation [6].

The aim of this phase I/II study was to determine the safety and efficacy of radiofrequency ablation (RFA) of early breast carcinomas using saline-cooled electrodes. Our secondary goals were to determine the size, configuration and pathological features of acute RF ablative treatment of breast carcinomas.

## Patients and methods

### Patients

All patients had a prior histological diagnosis of breast cancer established by stereotactic or US-guided core biopsy. Core biopsy had to be adequate for routine pathological evaluations (grade, estrogen receptor, progesterone receptor, Her 2-neu) because after RF ablation has been performed, viable tumor may not be available for these analyses.

Eligibility criteria included age between 20 and 90 years and tumor size $\leq$3.0 cm in diameter on US examination. Patients were excluded if there was evidence of diffuse calcification suggestive of extensive multifocal ductal carcinoma in situ of more than 3.0 cm in size.

MRI was performed on all patients to evaluate the lesions more precisely and compared with the results of RF ablation. Patients treated with preoperative chemotherapy were excluded. This study was approved by the National Cancer Center, Japan Institutional Review Board, and all patients provided written informed consent.

### Treatment

All patients underwent breast US and MRI preoperatively to determine if the tumor was visible in order to facilitate US-guided RF ablation. The patient could elect to undergo either a lumpectomy or a mastectomy as in both situations the RF ablated tissue would be available for pathological review. Sentinel lymph node biopsy (SLNB) was performed for axillary staging. Tracers for SLNB were injected into the subareolar parenchyma to prevent the interference of air/fluid with intra-operative US imaging.

After general anesthesia was induced and SLNB was completed, the breast tumor was identified with intraoperative US using the Toshiba Aplio XG SSA-790A (Toshiba Medical Systems Corporation, Otawara, Japan) with a PLT-1204AT (2D, 12 MHz) and a PLT-1204MV (4D, 14 MHz) probe. Under US guidance, the 17-gauge Valleylab™ RF Ablation System with Cool-tip™ Technology (Covidien, Energy-Based Devices, Interventional Oncology, Boulder, CO) was inserted in the center of the tumor (Fig. 1). With US imaging in the two planes, we ensured that the electrode was located in the center of the lesions using a linear 2D probe for the vertical image and 4D probe for the coronary image (Fig. 2). In all cases, a 2-cm active tip electrode was used. Before ablation, we injected 20 to 40 ml of 5% glucose to avoid skin or muscle burn. The needle electrode was attached to a 500-kHz monopolar RF generator capable of producing 200-W power. Grounding was achieved by attaching two grounding pads to the patient's thighs before the producer. Tissue impedance was monitored continuously using circuitry incorporated into the generator. A peristaltic pump (Watson-Marlow, Medford, MA) was used to infuse 0°C normal saline solution into the lumen of the electrode at a rate sufficient to maintain a tip temperature of 15–25°C.

RF energy was applied to tissue with an initial power setting of 10 W and subsequently increased with increments of 5 W each minute to a maximum power of 55 W. Saline circulating internally within the electrode cools the adjacent tissue, maximizing energy deposition and reducing tissue charring. The power setting was left at this point until power 'rolloff' occurred. Power rolloff implies that there is an increase in the tissue impedance caused by loss of sodium chloride, which occurs with tissue coagulation around the monopolar electrode. When this occurs, the power generator will shut off, stopping the flow of current and further tissue coagulation. After waiting 30–60 s, the second phase was started at 75% of the last maximum power until a second rolloff occured. The appearance and progression of hyperechogenicity on US were used to guide the therapy. Radiofrequency was applied until the tumor was completely hyperechoic (Fig. 3). To minimize thermal injury to the skin, sterile ice packs were placed on the breast during the ablation procedure (Fig. 4). Following RF ablation, standard tumor resection was achieved with either a wide local excision or mastectomy according to the preference of the patient. The surgical specimen was obtained and immediately sent fresh to the pathology department.

### Pathological evaluation

#### *Frozen section*

Specimens resected by the surgeons were submitted to the pathologists for nicotinamide adenine dinucleotide

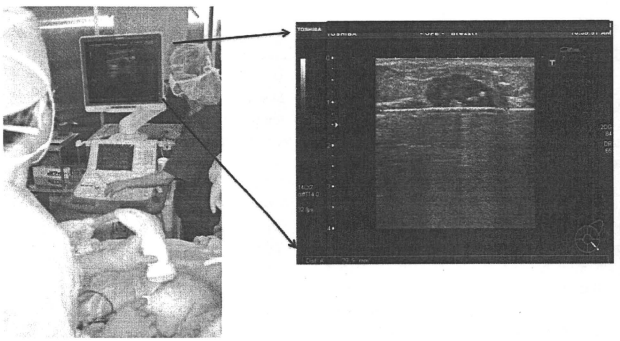

**Fig. 1** Technique for performing breast radiofrequency ablation (RFA). Under ultrasound guidance the RF electrode is percutaneously inserted into the breast tumor. The needle is seen transversing the target tumor

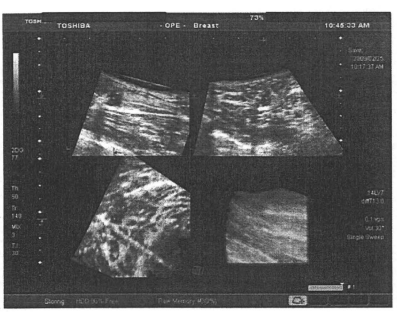


**Fig. 2** Confirmation of the location of the needle using a 4D probe. With ultrasound imaging in the two planes, we ensured that the electrode was located in the center of the lesions using a linear 2D probe for the vertical image and 4D probe for the coronary image

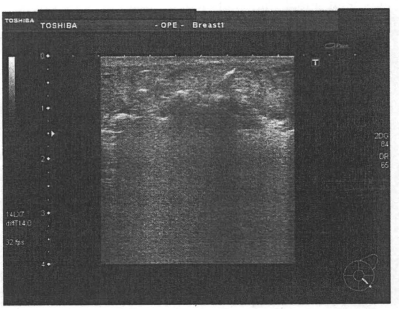


**Fig. 3** Intraoperative breast ultrasound. Radiofrequency was applied until the tumor was completely hyperechoic

(NADH) diaphorase cell viability analysis and routine histopathological examination. A tissue slice including the representative cut surface of the tumor and non-ablated mammary glands was removed and subjected to frozen section preparation.

One to two pieces of representative tumor tissue and another piece of non-ablated mammary gland were snap frozen in liquid nitrogen and cut into 5-μm-thick sections using a cryostat (Shiraimatsu, Tokyo, Japan). One of the sections was stained with H&E and was microscopically confirmed to contain the representative tumor tissue and non-ablated mammary gland tissue. Other sections were stored at −20°C until NADH diaphorase assay.

**Fig. 4** Skin protection. Skin is protected by the placement of an ice pack during the RFA procedure

*Histological analysis*

From residual tissue specimens, an entire representative cut surfaces of the ablated tumor and surrounding tissue were taken as tissue blocks for histopathological examination. The blocks were formalin-fixed, paraffin-embedded and cut into 3- to 4-μm-thick sections. These sections were stained with HE. Histopathologically, the viability of tumors was evaluated in consideration of thermocautery artifacts. When the degeneration was marked in cancer cells, the effect of thermocautery was effective. The tumor area with marked degeneration was calculated for each case.

Immunohistochemically, expression of estrogen receptor (ER, clone ID5 clone, Dako, Glostrup, Denmark), progesterone receptor (PR, clone IA6, Dako) and HER2 (Herceptest, Dako) were examined. For ER and PgR, a tumor was judged as positive if 10% or more of the tumor cells showed positive nuclear immunoreactions irrespectively of the intensity of the immunoreactions. For HER2, judgment about immunoreactions was made according to the recommendations of the ASCO/CAP guidelines.

*NADH diaphorase cell viability analysis*

The enzyme histochemical analysis of cell viability was performed based on the reduction of nitroblue tetrazolium chloride, a redox indicator, by NADH diaphorase, resulting in an intense blue cytoplasmic pigmentation. The activity of this enzyme has been shown to subside immediately upon cell death. For this analysis, 5-μm cryostat-cut unfixed sections were placed in a coprin jar and incubated in 0.05 M tris-buffered saline (TBS, pH 7.4) containing 500 mg/l tetranitro blue tetazolium and 800 mg/l β-NADH (Sigma-Aldrich Corp., St. Louis, MO) for 30 min at 37°C. Thereafter, the sections were fixed in 10% formalin for 30 min, washed with distilled water for 2 min and mounted with a cover glass. Based on the area of cells with blue cytoplasmic staining, the viability of tumor cells and non-ablated mammary gland cells as control was evaluated.

## Results

Fifty patients were enrolled in the study, and 49 completed RF ablation therapy. For one patient, the ablation system had some trouble, and we decided not to proceed with the therapy. The patient demographics of the 49 patients who received the proposed RF ablation therapy are shown in Table 1. The median age was 61 years (range 36–82). The median breast tumor size based on the ultrasonographic maximum dimension was 1.70 cm (range 0.5–3.0). The histology was invasive ductal carcinoma for 43 patients (88%).

**Table 1** Patient demographics of 49 patients

| | Number of patients |
|---|---|
| Age (years) | |
| Median | 61 |
| Range | 36–82 |
| Method of diagnosis | |
| Mammgoram screening | 32 (65%) |
| Palpable mass ± mammogram | 17 (35%) |
| Tumor classification | |
| Tis | 1 (2%) |
| T1 | 34 (69%) |
| T2 | 14 (29%) |
| Tumor location | |
| Upper outer | 18 (37%) |
| Lower outer | 5 (10%) |
| Upper inner | 18 (37%) |
| Lower inner | 7 (14%) |
| Central | 1 (2%) |
| Tumor size on US (cm) | |
| Median | 1.70 |
| Range | 0.5–3.0 |
| Tumor size on MRI (cm) | |
| Median | 1.50 |
| Range | 0.7–4.5 |
| Lymph node status | |
| N0 | 44 (90%) |
| N1 | 5 (10%) |

RF ablation time ranged from 3–18 min (mean 8.7 min). Mean tumor impedance was 195.1 Ω, and for 4 of 49 patients, there was a reduction in the impedance during treatment by a mean of 53.4 Ω.

A median of one cycle and a mean power of 48.5 W (range 5–118 W) were used to achieve tumor ablation.

RFA of the breast tumor was monitored with ultrasonography every 3 min.

In 49 patients, as tumor heating around the multiple array electrodes developed, an ill-defined, hyperechoic zone developed. The size of the ablation measured by ultrasonography ranged from 15 to 50 mm (mean 27.3 mm).

RFA-related adverse events were observed in five cases (10%): two with skin burns and three with muscle burns. The entire skin burn area was excised during the breast tumor resection, and the patient had no further sequelae. These events occurred in initial cases. So, in order to avoid these burns, 10 ml of 5% glucose was injected between the skin and tumor, and also between the muscle and tumor. Since then, no skin burns have been observed.

There was no bleeding from the needle track upon removal of the RFA needle electrode in any of the 49 patients.

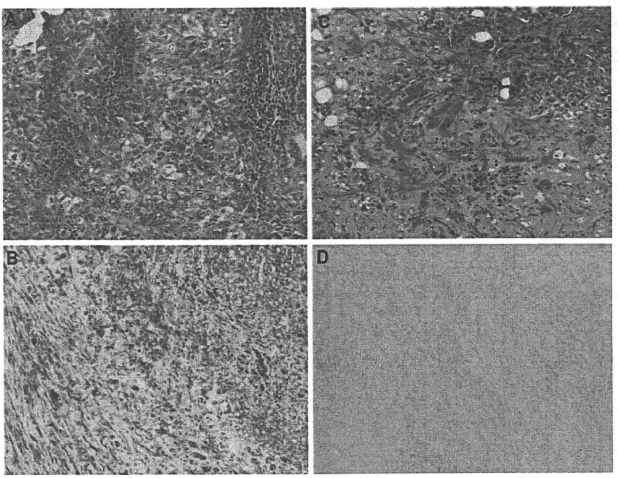


**Fig. 5** NADH viability study. **a** H&E section of non-ablated breast tumor; **b** NADH viability study of non-ablated breast tumor T; **c** H&E section of ablated breast tumor; **d** NADH viability study demonstrating non-viable ablated tumor (magnification ×200)

Surgical resection consisted of total mastectomy in 27 patients, whereas 22 patients underwent wide local excision. In the early stages of this study, we selected the patients with small breast cancers who prefered to be treated by mastectomy.

On H&E examination, the tumor architecture was maintained despite ablation, which allowed the pathological size to be assessed accurately. The RFA-treated carcinomas showed a range of pathological findings. All of the treated tumors showed elongated nuclei with smudged chromatin (Fig. 5c). All cases showed extensive electrocautery changes with densely eosinophilic stromas.

In resected samples ablated with a 2.0-cm active tip of the electrode, the results of H&E and NADH examination showed that the mean diameter of the major axis was 3.0 cm (range 0–6.6 cm) and of the minor axis 2.2 cm (range 0–6.6 cm) (Table 2).

NADH viability staining was available for 26 patients, and in 20 (76.9%), there was no evidence of viable malignant cells (Fig. 5d).

Among cases of tumor diameter less than 2 cm in pathological examination, the NADH viability staining was available for 22 patients, and in 20 (90.9%), there was no evidence of viable malignant cells. The two viable cases were due to insufficient ablation; the reason for one case was a defective device and for another case was that the impedance was too high for the tumor to be ablated completely.

In H&E examinations, all tumors diagnosed with non-viability with NADH staining had confirmed changes with characteristics, i.e., amorphism, in the interstitial cells, linear form, rarefaction and inspissation in the nucleus of epithelial cells, etc.

Among most of the cases with viable malignant cells diagnosed with NADH staining, each tumor diameter was nearly 3 cm. Only one case had incomplete ablation of the index tumor because the tumor was eccentric within the RFA zone.

In total, on H&E and or NADH staining, 18 patients (37%) in 49 RFA cases had some viable invasive or in situ disease seen in the surgical excision specimen.

Table 3 shows treatment results depending on the pathological tumor size, including both invasive and intraductal lesions measured in surgical excision specimens. Out of 29 cases with tumor diameters $\leq$2 cm in pathological examination, 25 (86%) had confirmed complete ablation. In 20 cases of tumor diameter >2 cm, only 6 cases (30%) showed confirmed complete ablation. Table 4 indicates that the treatment result also depended on the existence of an extended intraductal component (EIC) of the tumor in the surgical excision specimen. In 26 cases of tumor without EIC in pathological

**Table 2** Pathological findings for 49 patients

| | Number of patients |
|---|---|
| Tumor type | |
| Invasive ductal | 43 (88%) |
| Invasive lobular | 1 (2%) |
| Mucinous | 2 (4%) |
| Medullary | 2 (4%) |
| DCIS | 1 (2%) |
| Tumor grade | |
| 1 | 22 (45%) |
| 2 | 16 (33%) |
| 3 | 11 (22%) |
| Pathological nodal status | |
| Negative | 39 (80%) |
| Positive | 10 (20%) |
| Pathologic tumor size (cm) | |
| Median | 1.7 |
| Range | 0.1–8 |
| Extended intraductal component (EIC) | |
| Present | 23 (47%) |
| Absent | 26 (53%) |
| Pathologic response to RFA | |
| Longest diameter of ablation zone (cm) | |
| Median | 3.0 |
| Range | 0–6.6 |
| Shortest diameter of ablation zone (cm) | |
| Median | 2.2 |
| Range | 0–6.6 |
| Incomplete tumor ablation | 19 (39%) |
| Residual INV | 8 (16%) |
| Residual DCIS | 11 (23%) |

*RFA* Radio frequency ablation

**Table 3** Correlation between pathological tumor size and tumor ablation

| Pathological tumor size (cm)[a] | No. of patients | Complete tumor ablation (%) | Incomplete tumor ablation (%) |
|---|---|---|---|
| ≤2 | 29 | 25 (86) | 4 (14) |
| >2 | 20 | 6 (30) | 14 (70) |

[a] Size of invasive and DCIS

**Table 4** Correlation between existence of EIC and tumor ablation

| | No. of patients | Complete tumor ablation (%) | Incomplete tumor ablation (%) |
|---|---|---|---|
| EIC present | 23 | 9 (39) | 14 (61) |
| EIC absent | 26 | 22 (85) | 4 (15) |

*EIC* Extended intraductal component

examination, 22 (85%) had confirmed complete ablation. In 23 cases of tumor with EIC, only 9 (39%) had confirmed complete ablation.

According to these results, pre-RFA MRI detection with ultrasonography should be examined to detect the EIC of the tumor, and appropriate cases for RFA must be determined.

## Discussion

Radiofrequency ablation is mainly used in clinical practice to treat unresectable hepatic tumors, and so far experience with breast carcinomas is limited [7–12].

RFA causes local tumor cell destruction by thermal coagulation and protein denaturation [5, 7, 13]. The higher the target temperature, the less exposure time is needed for cellular destruction [14, 15]. Cell death occurs above 45–50°C approximately. The target temperature mostly used at the tip of the prongs was 95°C and was maintained around 15 min [16]. It is conceivable that this setting could result in melting the fatty tissue, with bad cosmetic results. However, the lesions might be destroyed equally well with a lower target temperature and shorter ablation time [8].

Clearly, more research on the radiofrequency dose and effect is necessary to optimize RFA in breast carcinomas.

The shape, size and design of the RF electrode determined the shape of the ablation zone and, in the end, the success of the procedure. Because the size of the thermal lesion is limited using a single-needle electrode, multiarray electrodes have been developed that can produce thermal lesions of 3–5 cm in diameter.

In our trials, the ablation zone with a 2-cm active tip of the electrode had the following characteristics: the mean diameter of the major axis was 3.0 cm (range 0–6.6 cm) and that of the minor axis was 2.0 cm (range 0–6.6 cm).

However, some studies reported the distance between the tumor and the skin and the chest wall should be at least 1 cm because of possible burning of normal tissue. Lateral compression of the breast during the entire ablation procedure or ice cooling in cases of borderline distance to the skin is also essential to prevent possible skin burns [7, 8].

However, using a 5% glucose injection between the skin and tumor, and between the chest wall and tumor, and cooling skin with ice in order to avoid these burns, a tumor diameter less than 1 cm could be achieved with RFA.

The difficulty in assessing the margin of the ablated lesions is a limitation in all percutaneous ablation techniques. To minimize the risk of local recurrence and to make sure the whole tumor and safe margin are ablated, the lesions need to be excised with a rim of at least 1 cm.

After excision, tumor viability is tested by NADH diaphorase. Almost every study described immediate

excision of the ablated lesion [8, 10–12]. Burak et al. and Hayashi et al. [1, 9] had an interval of 1–3 weeks before excising the ablated zone. It was hypothesized that due to the effect of local vessel thrombosis and necrosis of surrounding tissue, the ablated zone expands in the period of time and provides a more accurate excision. In the end, the two trials did not have higher percentages of complete tumor ablation compared to the other studies, and it was concluded that an interval time between ablation and excision of the tumor might not be necessary [7, 9].

In cases of tumor diameter less than 2 cm, the NADH viability staining was available for 22 patients, and in 20 (90.9%), there was no evidence of viable malignant cells. The other two viable cases were due to insufficient ablation; the reason for one case was a defective device and for another case that impedance was too high for the tumor to be ablated completely. Breast cancer tissue is usually composed of tumor, normal tissue, fat, vessels, etc., and shows heterogeneity. The fat tissue has one of the highest electrical resistances. High resistance mean less effect from electrical power, such as radiofrequency. Therefore, we suspect that in our cases the component with high impedance against RFA might be fatty.

Up until now, only one pilot study has been performed that tested RFA in three elderly patients with breast cancer without excision of the ablated zone [17]. All three patients completed the treatment without complications, and after 18 months of follow-up, no recurrence had occurred. In the future, if RFA is to be used as a replacement for surgery, CNB might also be an option to confirm successful ablation. Fornage et al. suggested that multiple core-needle biopsies through the ablated lesion and its periphery should be obtained 3–4 weeks after the RFA procedure.

An indication for RFA can be early breast cancer ($T \leq$ 2 cm). In 29 cases of tumor diameter $\leq$2 cm, 25 (86%) were confirmed to have complete ablation (Table 3). In 26 cases of tumors without EIC in pathological examination, 22 (85%) were confirmed to have complete ablation. In 23 cases of tumor with EIC, only 9 (39%) were confirmed to have complete ablation. According to MRI detection, tumor diameter and the EIC could be evaluated more accurately. Appropriate cases for RFA should be selected deliberately after enough diagnosing with US and MRI detection concerning the diameter, type, EIC, multiple lesions, etc.

The optimal conditions for RFA correlate to results under the following conditions: (1) tumor diameter <2 cm diagnosed with US and (2) <2 cm except for multiple lesions and extended intraductal spread of lesions of more than 2 cm diagnosed with MRI detection.

Also, in two cases, the tumor body could not be ablated sufficiently. Effects of RFA depend on tissue resistivity, so fatty tissue and tumor components can affect these effects. Components of breast carcinoma are different for each patient, and further studies are needed. In cases in which the initial resistance is too high and rolloff occurs immediately, as our study showed, the target temperature cannot be reached, and procedures should be changed from RFA to lumpectomy for the patients' safety. The reasons for these incidents need to be examined with resected samples.

In Japan, RFA is a popular treatment method for liver cancer.

Half of liver cancer patients are treated by RFA. This system is familiar to many physicians even in local hospitals and clinics.

Although cryoablation and the HIFU have not been approved by the Japanese government, only RFA has been approved and has the possibility to be admitted as an option for local treatment.

RFA seems to be a promising new tool for a minimally invasive procedure for small breast carcinomas. However, follow-up data regarding the local effects on the surrounding breast tissue or recurrence rates are hardly available. Further research will be necessary to establish the optimal technique and to demonstrate the long-term oncological and cosmetic effects of RFA.

**Acknowledgments** This study was supported by a grant from the Clinical Research for Development of Preventive Medicine and New Therapeutics of Health and Labor Science Research of Japan.

## References

1. Fisher B, Remand C, Poisson R, et al. Eight year results of a randomized clinical trail comparing total mastectomy and lumpectomy with or without radiation in treatment of breast cancer. N Engl J Med. 1989;320:822–8.
2. Veronessi U, Salvatori B, Luini A, et al. Conserving treatment of early breast cancer: long term results of 1232 cases treated with quadrantectomy, axillary dissection and radiotherapy. Ann Surg. 1990;211:250–9.
3. Olsen O, Gotzche PC. Cochrane review on screening for breast cancer with mammography. Lancet. 2001;358:1340–2.
4. Vreling C, Collette L, Fourquet A, et al. The influence of patient tumor and treatment factors on the cosmetic results after breast-conserving therapy in the EORTC7 'boost vs. no boost' trial. EORTC Radiotherapy and Breast Cancer Cooperative Groups. Radiother Oncol. 2000;55:219–32.
5. Singletary SE. Minimally invasive techniques in breast cancer treatment. Semin Surg Oncol. 2001;20:246–50.
6. Cady B, Stone MD, Schuler JG, et al. The new era in breast cancer. Invasion, size, and nodal involvement dramatically decreasing as a mammographic screening. Arch Surg. 1996; 131:301–8.
7. Burak WE, Agnese DM, Pozoski SP. Radiofrequency ablation of invasive breast carcinoma followed by delayed surgical excision. Cancer. 2003;98:1369–76.
8. Fornage BD, Sneige N, Ross MI. Small ($\leq$2 cm) breast cancer treated with ultrasound-guided radiofrequency ablation. Am J Surg. 2004;231:215–24.